Journal of Manufacturing Processes 76 (2022) 752–757

Contents lists available at ScienceDirect

Journal of Manufacturing Processes

journal homepage: www.elsevier.com/locate/manpro

Electrostatically-assisted direct ink writing with superior speed and resolution

J. Plog [a], X. Wang [a], Y. Pan [a,*], A.L. Yarin [a,b,**]

[a] Department of Mechanical and Industrial Engineering, University of Illinois at Chicago, 842 W. Taylor St., Chicago, IL 60607-7022, USA
[b] School of Mechanical Engineering, Korea University, Seoul 136-713, Republic of Korea

ARTICLE INFO

Keywords:
Direct ink writing
Fast printing
Micromanufacturing
Electric field

ABSTRACT

Here, the addition of an electrode to the printhead in direct-ink-writing (DIW) generates an electric field (E.F.) between the electrode and the printing nozzle. The extruded ink, as an ionic conductor, is then pulled by the Coulomb force in the direction of printing, resulting in much faster writing speeds and much thinner traces (lines) and smaller widths. Limitations in speed and resolution are practically removed here because the integration of an electrode into the printhead allowed successful prints at 13.2 m/s, ~13 times faster than in other published works, as to our knowledge, and almost ~30 times faster than in most commercial printers, which are limited to 0.5 m/s. A print speed of 13.2 m/s is reached in the present work, which unlocks the speed restrictions associated with DIW and holds great promise for new design opportunities. In addition, by means of E.F., an improved resolution up to 35 μm line width has been achieved here. It should be emphasized that the high printing speed and fine resolution demonstrated in this work are still not the physical limits of the method but rather only the restrictions imposed by the present experimental setup.

1. Introduction

Direct ink writing (DIW) is a flexible additive manufacturing (AM) technique proving advantageous in widespread fields from wearable electronics, structural composites, soft robotics to artificial organs [1–4]. While known to be a relatively slow AM technique [5,6], the primary strength of DIW is the diversity of available materials [7] and capability of printing metals, polymers, ceramics and bio-gels, etc. [8–11] into complex 2D or 3D patterns. Consistent with other AM techniques, DIW also demonstrates freedom of structural design and reduced concept-to-completion time, while concurrently keeping waste to a minimum [12–14]. Synonymous with Robocasting and robotic material extrusion, DIW is essentially the ink deposition over various substrates following a preset pattern or layout [15].

As DIW technologies proliferate within an evolving industry, manufacturers demand ever-increasing throughput as modern applications simultaneously evolve to both minimum and maximum printing extremes (i.e., one industry path may choose to print on micro- or even nano-scale while the other path may 3D print an entire grand-scale 'house'). Even though the extremes are in many aspects polar, one similarity the two manufacturing directions share is the overall complexity and length of the tool paths which are the sequential physical motions the printhead follows. The length of this tool path is easy to see on the grand scale of a 3D printed 'house', albeit it may not be so intuitively recognizable on a small print of high-resolution how far the printhead mechanically translates. Comprised often of hundreds of thousands of coded lines, tool paths of a complex print may place the smallest possible lines (typically 50–200 μm) next to each other to form a thin plane. These thin planes are then stacked to form a volume, once again re-emphasizing the lengthy process where prints may take days [16].

In today's metaphoric gold rush of AM, speed is valued on a similar magnitude as resolution and cost. One known problem in DIW, and most AM systems, is that an increased velocity between substrate and nozzle directly correlates with an increase in manufacturing defects [17]. These defects may include, but are not limited to, discontinuous lines, bulging, liquid puddles, splashing or coffee ring effect [18–26]. As to our knowledge, there are not many publications devoted to increasing the printing speed or reducing the associated detrimental effects. It was demonstrated that electrowetting helps to reduce bulging in prints of

* Corresponding author.
** Correspondence to: A.L. Yarin, Department of Mechanical and Industrial Engineering, University of Illinois at Chicago, 842 W. Taylor St., Chicago, IL 60607-7022, USA.
E-mail addresses: yayuepan@uic.edu (Y. Pan), ayarin@uic.edu (A.L. Yarin).

https://doi.org/10.1016/j.jmapro.2022.02.038
Received 17 December 2021; Received in revised form 10 February 2022; Accepted 18 February 2022
Available online 8 March 2022

low-viscosity liquids, which could potentially lead to faster prints [7]. Electrohydrodynamic (EHD) jetting resulted in writing speeds up to 0.5 m/s, albeit only for lines less than 2 mm in length [27]. 'Very high translation speeds', up to 1 m/s (in a circular pattern), were reported too, but the observed print quality and stability were greatly affected by the ink viscosity [28]. In recently published work, the DIW of cylindrical lattice structures resulted in meters upon meters of printed lines wrapping around a cylinder printed with a speed around 0.01 m/s [6]. The above-mentioned state of the art highlights the need for much higher DIW's printing speeds required to match the demand from industrial applications. When current standards measure tool paths in meters or kilometers, yet the production of lines proceeds in millimeters or centimeters per second, the situation can be characterized as a significant disconnect between desired and actual print times.

In previous work of this group, it was found that a commercial DIW robot's operating range of 0–0.5 m/s be more than adequate as most prints failed at 0.1–0.2 m/s with no E.F. applied. With the introduction of our E.F.-assisted printing process (charged electrode near the printhead), this 0.5 m/s maximum was easily reached while still producing continuous trace lines at fine resolutions, and meanwhile minimizing the defects from consequent instabilities [29]. Note that a comprehensive theoretical model of the DIW process (including the E.F.-assisted printing process) was also given in our previous work [29].

Present work aims to address the above-mentioned challenges while pushing DIW's speed to a much higher limit for continuous translating deposition achievable in the current setup. Here, the conventional DIW process is modified with a strategically applied E.F. set to pull the inkjet footprint on the moving substrate in the direction opposite to that of the relative substrate motion. In addition, the governing electrode is mounted on the printhead, and as a result, the effects of the E.F. do not diminish as the build height increases. The experimental setup is described in Section 2. The experiments performed to study the practical application of an E.F. to the jetting characteristics of DIW are presented and discussed in Section 3. Conclusions are drawn in Section 4.

2. Experimental setup

Several beneficial effects the E.F. exhibits while applied to a cylindrical jet being dispensed normally onto a horizontally translating substrate have been demonstrated in previous work of this group [29]. Because the current work aims primarily at increasing relative velocity between the printing nozzle and substrate, the previous setup was modified as sketched in Fig. 1. The defining improvements to this setup are a direct-drive motor with an increase in rotational velocity from 50 to 1000 rpm, an increase in drive spool diameter from 6 cm to 15 cm, and a ball-bearing belt support. The ball-bearing support was placed directly beneath the printing nozzle to help reduce undulations in the belt. This model setup kept the nozzle stationary and thus, helped facilitate the video recording of the DIW process.

Positively charging the governing electrode while simultaneously providing the ground to the printing nozzle, a high-voltage power supply was used to produce the forces acting on the inkjet, which is, as usual, an ionic conductor [30]. This resulting Coulomb force is opposite to the direction of the substrate motion and is always relatively uniform, even during substrate undulations, because it is generated by the printhead rather than the substrate. To create a driving pressure, a commercial pressure controller (Nordson Ultimus I) supplemented with 30-gauge stainless steel printing needles is being used in this setup. Such a system allowed for a well-defined pressure pulse (1–80 psi) to be applied to the ink within the needle for a specific time. It should be emphasized that the experiment was specifically designed to achieve both high speed and fine resolution of the print process. Because of this, smaller blunt-end needles of 30-gauge were chosen instead of the 27-gauge ones used in previous experiments of this group. Note that previously it was shown that needle diameter directly correlates with the maximum attainable printing speed, i.e., for a larger needle, faster prints will be achievable. However, even with the smaller needles chosen, the E.F. induced continuous prints at the present system's maximum belt velocity, which was much higher than before. The governing electrode was made of a 0.5 mm copper wire bent above the printing needle edge. Voltages applied to the governing electrode were in the 2.8–3.1 kV range with the E.F. strength increasing with the belt translational speed (i.e., ink writing speed). Because the reel-to-reel tape is pulled taut by the drag applied by the tensioning spool (cf. Fig. 1), the substrate tape takes the curved shape of the ball-bearing's surface over a minimal distance relative to the circumference of the bearing. This can be seen in magnified snapshots displayed in Figs. 3–6, albeit this curvature is not depicted or seen in the sketch in Fig. 1.

One important aspect linked to successful DIW implementation is the rheological behavior of the inks to be printed. Ideal DIW inks exhibit both shear-thinning and viscoelastic behavior easing the ink's flow through the nozzle. Three practically important inks were chosen for the experiments with high-speed DIW to evaluate the effect of surface tension and rheological properties characterized using shear and

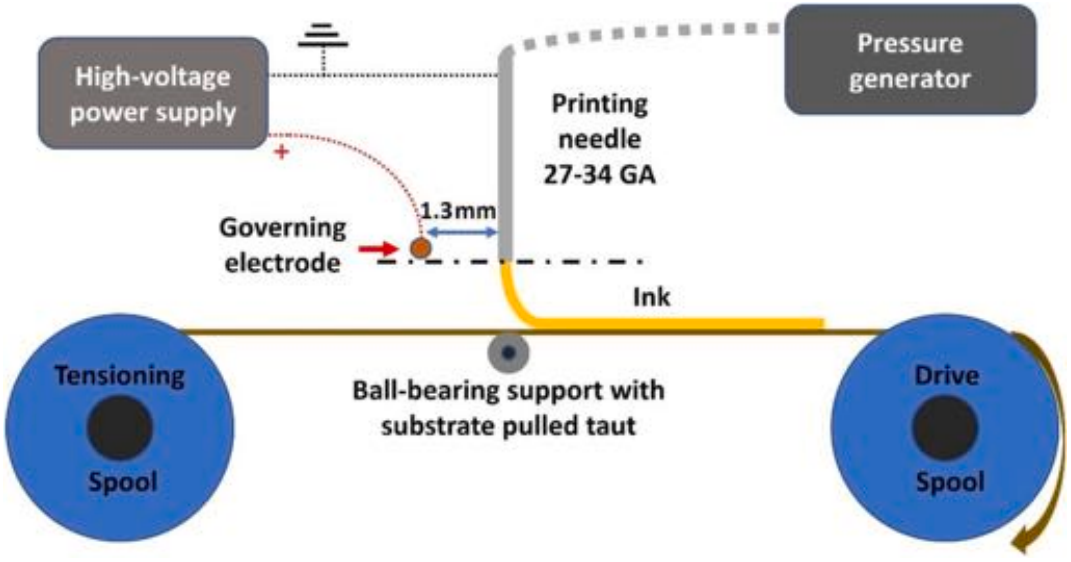

Fig. 1. Schematic of the experimental setup utilizing the perpendicular dispensing of a cylindrical jet onto a translating substrate. A voltage applied to the governing electrode is used to facilitate smooth and speedy ink deposition utilizing the E.F.

elongational flows [30], as listed in Table 1.

Rust-Oleum Stain & Polyurethane along with Tester's Model Paint were purchased from Amazon, while an unknown brand of solvent-based paint available in our lab was also subjected to testing. Even though the three inks chosen are relatively common in commercial and industrial applications, they are most likely perceived to most as unconventional DIW inks. Unlike the conventional DIW inks tested in previous works, intentions were to highlight that the applied E.F. can prove beneficial for practically all DIW-printable materials. The shear-viscosities of the three inks depicted in Fig. 2 reveal that Rust-Oleum stain and Tester paint reveal a certain degree of shear-thinning, whereas Solvent-based paint - a certain degree of shear-thickening (dilatancy). Note that dilatancy is highly undesirable in conventional DIW processes, which makes Solvent-based paint a challenge for printing at a high speed using the conventional DIW processes. In our work, this material printability challenge was addressed by applying the E.F., as the results discussed below reveal. It should be emphasized that the non-zero relaxation times of the order of 10^{-3}–10^{-2} s (cf. Table 1) measured using surface-tension-driven self-thinning of a liquid thread [30] reveal that all the three inks possess viscoelastic properties.

To apply E.F. in DIW, one 0.5 mm copper electrode was attached to a custom dielectric printhead by placing it in line with the printer's needle. To demonstrate the ultra-fast line printing, a continuous line was printed with and without the applied E.F. with line writing speeds in the 1.8–13.2 m/s range. The printing was limited to one direction-of-freedom like that used in offset newspaper printing. The continuous filament extrusion and deposition were captured using a high-speed CCD camera (Phantom VEO-E 340L) employing back-light shadowgraphy. All experiments were performed under ambient conditions.

3. Experimental results and discussion

All variables were kept constant with the exception of the applied E.F. Fig. 3 shows the dispensing of solvent-based paint extruded onto Mylar belt with and without the E.F. applied. Even at the lowest translational speed employed in current experiments (1.8 m/s), without the assistance of the E.F., the resulting print lines repetitively failed by either discontinuity or possessing widths that vary at unacceptable levels, as seen in the side and top views, respectively, in Fig. 3a and b. The side view in Fig. 3a highlights how the fluid collects between the nozzle and substrate while the top view in Fig. 3b reveals the outcome for the final printing line deposited. Fig. 3c captures a side view of the fixed printing state after the E.F. has been applied, and Fig. 3d shows the successfully printed line. These results are consistent with our previous results in [29], though now at a greater printing speed.

Then, the voltage to the brushed drive motor was increased to provide a belt translational speed of 5.18 m/s. It should be emphasized that most commercial DIW machines are limited to the speed of ~0.5 m/s, as without E.F. facilitation, continuous line printing would be impossible at higher speeds. However, with the E.F. altering the jet path, which, essentially, enhances wetting the substrate surface, the jet and advancing triple line are pulled toward the high-voltage electrode, thus, facilitating continuous prints at speeds 10 times higher than what industry previously considered the standard DIW speed. Fig. 4a reveals

Table 1
Surface tension and rheological properties of the three inks used in the high-speed DIW experiments. The values of the shear viscosity were measured at the lowest shear rates shown in Fig. 2.

	Surface tension (mN/m)	Shear viscosity (Pa s)	Relaxation time (s)
Solvent-based paint	30.9	0.8	0.006
Rust-Oleum stain	37.3	1.5	0.011
Tester paint	33.1	0.8	0.005

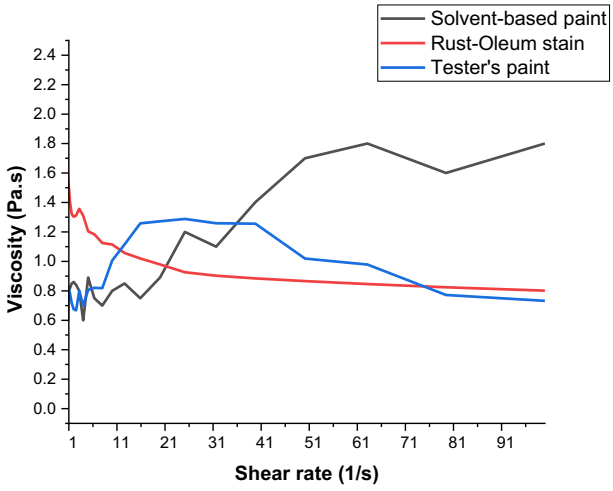

Fig. 2. Shear viscosity measured in simple shear flow for the three inks chosen for experiments. The shear flow measurements were performed using a commercial rotational rheometer (Kinexus Ultra+, NETZSCH Instruments).

how the ink is dispensed with a horizontal snapshot extracted from the high-speed recording of the print. Fig. 4b and Fig. 4c are both top views at different zooms highlighting the incredibly smooth edges of the dried printed lines. This is remarkable because the drive and tensioning wheels were 3D printed and not balanced leading to significant vibrations, which grew stronger as velocities increased and were detrimental to the printing process before applying the E.F. It should also be emphasized that this Solvent-based paint revealed dilatant properties (cf. Fig. 2), which is highly undesirable in DIW and is likely why this ink could not be faster printed, albeit (with the applied E.F.) still much faster than the current standard.

Two more inks were tested in further experiments. Both Rust-Oleum Stain & Polyurethane along with Testers Model Paint were used for printing. Fig. 5 depicts the side view (panel a) acquired during steady-state printing at 7.28 m/s of Rust-Oleum and the corresponding top view of the dried print (panel b). Again, a very smooth edge of the deposited material can be observed. Although not pictured, all three inks achieved successful line printing at similar velocities. Note the Rust-Oleum Stain exhibited the most-pronounced shear-thinning of the three inks tested.

By applying the maximum recommended voltage to the DC motor, a belt speed of 13.2 m/s was measured using the high-speed video with a resolution of 768 × 500 pixels shot at 7000 fps. As previously mentioned, the vibrations continuously increased with the rotational velocity and were quite noticeable in the video footage used to produce Fig. 6a. Fig. 6a depicts a side view of the printing process where even though the ink is stretched quite far along with the moving belt, the E.F. still pulls on the preceding lamina enough for a continuous print. The resolution (reduced line width) increased with printing speed (cf. Fig. 6b), similarly to the previous work of this group [29]. Typical DIW deposition at speeds below 0.25 m/s yields lines of width greater or similar to the nozzle from which they are printed. However, at ultra-fast DIW speeds achieved here with the help of E.F., the resulting dried printed line widths appear to be much less than the diameter of the printing nozzle. For instance, Fig. 6a shows a printing nozzle of a diameter ≈0.27 mm, while Fig. 6b shows the corresponding image of the printed line, which is ≈0.04 mm in width. Note that Fig. 6b does reveal a slight meandering, and it is unclear yet whether this was the result of the belt vibrations, hydrodynamic instability or some other unknown factors.

The results depicted in Figs. 4–6 show that the applied E.F. allows one to overbear any detrimental effects of dilatancy and high-viscosity, vibrations and capillary instability, and opens new opportunities in DIW

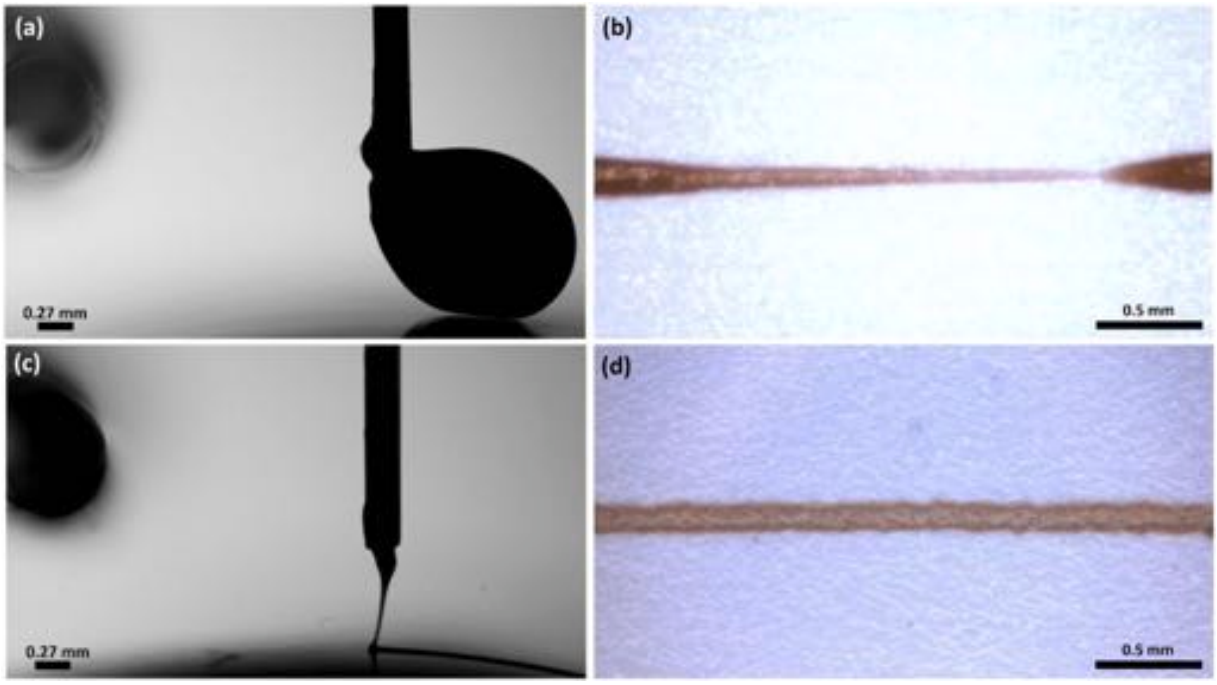

Fig. 3. Solvent-based paint extruded onto Mylar belt from the 30-gauge needle at 22 psi. (a) Side view and (b) top view of failed printing state without E.F. applied. (c) Side view and (d) top view with 2.8 kV applied to the governing electrode (seen to the left of the print needle in panels a and c, though not charged in the former). The printing speed is 1.8 m/s.

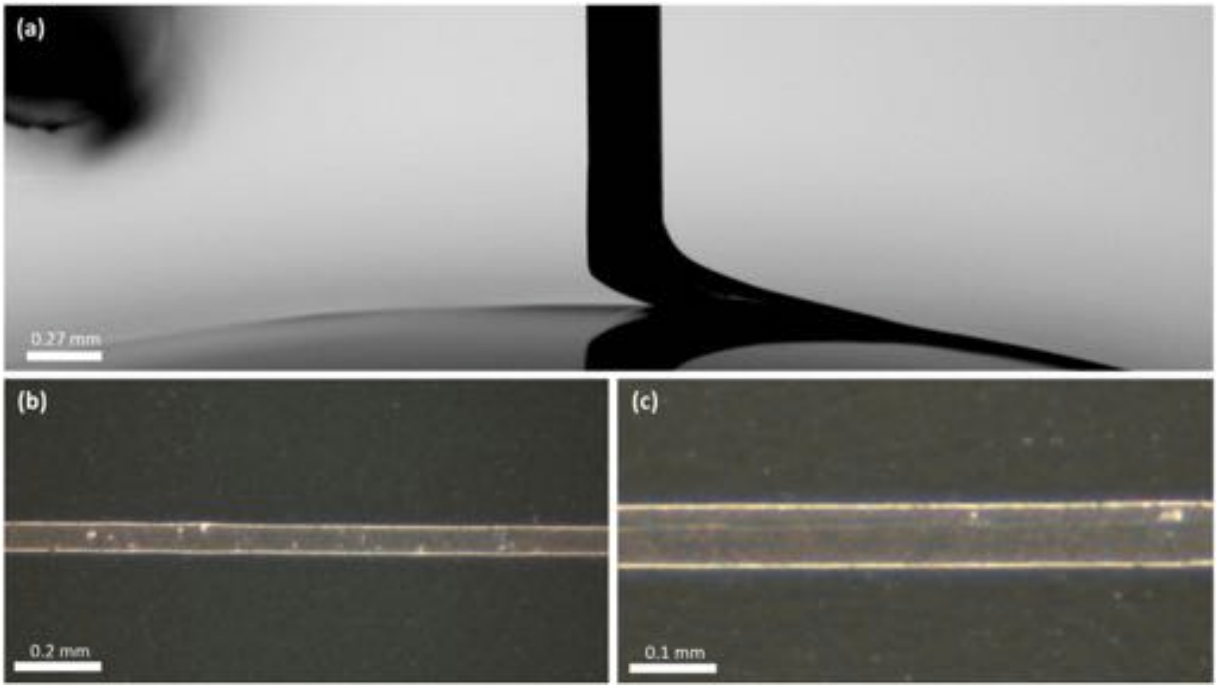

Fig. 4. Solvent-based paint extruded onto Mylar belt moving at 5.18 m/s from a 30-gauge needle at 60 psi with 3 kV applied to the governing electrode. (a) Side view (b) top view at 193× magnification. (c) Top view at 193× using digital zoom to highlight smooth edges.

not only bearing in mind the process speed but also when considering material choices.

4. Conclusion

The present experimental findings indicate great potential of the electric field (E.F.) application when an electrode is strategically positioned in the vicinity of a printing nozzle. This can significantly boost the printing speed and resolution associated with DIW processes by several orders of magnitude. Our approach has already been proven capable of printing on super-rough surfaces, while the present work shows that it helps to minimize the adverse effects of substrate vibrations. In addition to higher printable speeds and resolutions, accuracy E. F. and repeatability enhancements of printing are also demonstrated in

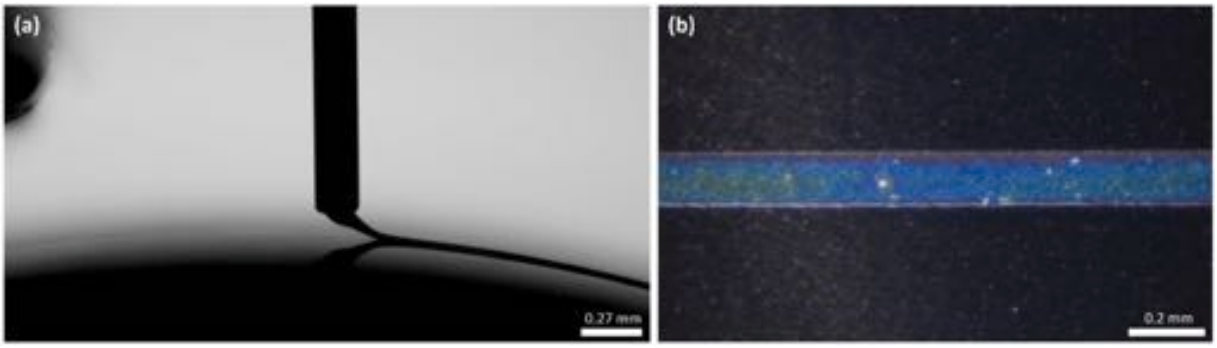

Fig. 5. Rust-Oleum Stain & Polyurethane extruded onto Mylar belt moving at 7.28 m/s from the 30-gauge needle at 75 psi with 3 kV applied to the governing electrode. (a) Side view. (b) Top view at 193× magnification.

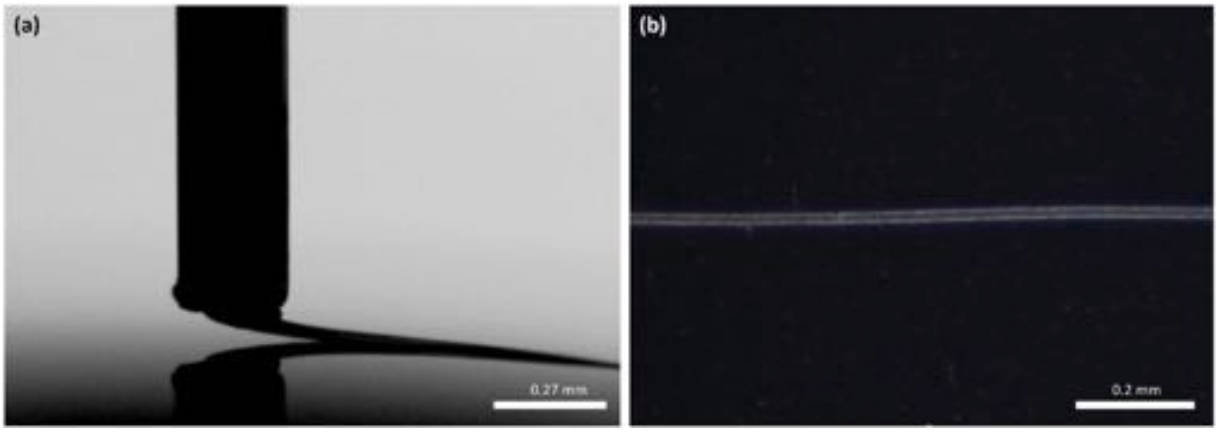

Fig. 6. Tester Model Paint extruded onto Mylar belt at 13.2 m/s from 30-gauge needle at 75 psi with 3.1 kV applied to the governing electrode. (a) Side view. (b) Top view at 193× magnification.

the present experiments. By applying E.F. and using a translating belt system placed below a fixed nozzle, an ink writing speed (i.e., printing speed) of 13.2 m/s was achieved. Particularly, by adding a single electrode near the nozzle, printing speeds were increased by a factor of 30 compared to unassisted prints. The current approach reveals experimentally its ability to significantly increase ink writing speed while minimizing the undesirable instabilities associated with increased velocities. This E.F.-based approach thoroughly addressed the common trade-off between printing speed and printing quality in DIW processes.

Declaration of competing interest

The authors declare that they have no known competing financial interests or personal relationships that could have appeared to influence the work reported in this paper.

Acknowledgment

This project was partially supported by National Science Foundation (NSF) Grant 1825626.

References

[1] Jiang Y, Cheng M, Shahbazian-Yassar R, Pan Y. Direct ink writing of wearable thermoresponsive supercapacitors with rGO/CNT composite electrodes. Adv Mater Technol 2019;4:1900691.
[2] Yang Y, Chen Z, Song X, Zhang Z, Zhang J, Shung KK, Chen Y. Biomimetic anisotropic reinforcement architectures by electrically assisted nanocomposite 3D printing. Adv Mater 2017;29:1605750.
[3] Kim Y, Yuk H, Zhao R, Chester SA, Zhao X. Printing ferromagnetic domains for untethered fast-transforming soft materials. Nature 2018;558:274–9.
[4] Noor N, Shapira A, Edri R, Gal I, Wertheim L, Dvir T. 3D printing of personalized thick and perfusable cardiac patches and hearts. Adv Sci 2019;6:1900344.
[5] Rocha VG, Saiz E, Tirichenko IS, García-Tuñón E. Direct ink writing advances in multi-material structures for a sustainable future. J Mater Chem A 2020;8:15646–57.
[6] Biasetto L, Franchin G, Elsayed H, Boschetti G, Huang K, Colombo P. Direct ink writing of cylindrical lattice structures: a proof of concept. Open Ceramics 2021;100139.
[7] Jiang Y, Wang X, Plog J, Yarin AL, Pan Y. Electrowetting-assisted direct ink writing for low-viscosity liquids. J Manuf Process 2021;69:173–80.
[8] Kalsoom U, Nesterenko PN, Paull B. Recent developments in 3D printable composite materials. RSC Adv 2016;6:60355–71.
[9] Hon KKB, Li L, Hutchings IM. Direct writing technology—advances and developments. CIRP Ann 2008;57:601–20.
[10] Zhu C, Han J, Duoss B, Golobic A, Kuntz J, Spadaccini M, Worsley M. Highly compressible 3D periodic graphene aerogel microlattices. Nat Commun 2015;6:1–8.
[11] Fu K, Wang Y, Yan C, Yao Y, Chen Y, Dai J, Hu L. Graphene oxide-based electrode inks for 3D-printed lithium-ion batteries. Adv Mater 2016;28:2587–94.
[12] Gibson IG. Additive manufacturing technologies 3D printing, rapid prototyping, and direct digital manufacturing. 2015.
[13] Pei E, Monzón M, Bernard A. Additive manufacturing-developments in training and education. London: Springer International Publishing; 2019.
[14] Srivatsan T, Sudarshan S. Additive manufacturing: innovations, advances, and applications. CRC Press; 2015.
[15] Chrisey D, Pique A. Introduction to direct-write technologies for rapid prototyping. In: Direct-Write Technologies for Rapid Prototyping Applications: Sensors, Electronics, and Integrated Power Sources; 2002. p. 1–16.
[16] Feilden E, Blanca E, Giuliani F, Saiz E, Vandeperre L. Robocasting of structural ceramic parts with hydrogel inks. J Eur Ceram Soc 2016;36:2525–33.
[17] Povarov O, Nazarov O, Ignat'evskaya L, Nikol'skii A. Interaction of drops with boundary layer on rotating surface. J Eng Phys 1976;31(1453–1456):395–414.
[18] Boley J, White E, Chiu G, Kramer R. Direct writing of gallium-indium alloy for stretchable electronics. Adv Funct Mater 2014;24:3501–7.
[19] Yang X, Chhasatia V, Shah J, Sun Y. Coalescence, evaporation and particle deposition of consecutively printed colloidal drops. Soft Matter 2012;8:9205–13.

[20] He M, Zhang Q, Zeng X, Cui D, Chen J, Li H, Wang J, Song Y. Hierarchical porous surface for efficiently controlling microdroplets' selfremoval. Adv Mater 2013;25:2291–5.
[21] Kuang M, Wang L, Song Y. Controllable printing droplets for high resolution patterns. Adv Mater 2014;26:6950–8.
[22] Singh M, Haverinen H, Dhagat P, Jabbour G. Inkjet printing process and its applications. Adv. Mater. 2010;22:673–85.
[23] Jiang Y, Hu S, Pan Y. A normalized trace geometry modeling method with bulgefree analysis for direct ink writing process planning, 3D print. Addit Manuf 2018;5:301–10.
[24] Wang J, Zheng Z, Li H, Huck W, Sirringhaus H. Dewetting of conducting polymer inkjet droplets on patterned surfaces. Nat Mater 2010;3:171–6.
[25] Vunnam S, Ankireddy K, Kellar J, Cross W. Surface modification of indium tin oxide for direct writing of silver nanoparticulate ink micropatterns. Thin Solid Films 2013;531:294–301.
[26] Zheng Y, Zhang Q. Pervasive liquid metal based direct-writing electronics with roller-ball pen. AIP Adv 2013;3:112117.
[27] Liashenko I, Rosell-Llompart J, Cabot A. Ultrafast 3D printing with submicrometer features using electrostatic jet deflection. Nat Commun 2020;11:753.
[28] LeBlanc K, Niemi S, Bennett A, Harris K, Schulze K, Sawyer W, Angelini T. Stability of high-speed 3D printing in liquid-like solids. ACS Biomater Sci Eng 2016;2:1796–9.
[29] Plog J, Jiang Y, Pan Y, Yarin AL. Electrostatically-assisted direct ink writing for additive manufacturing. Addit Manuf 2021;39:101644.
[30] Yarin AL, Pourdeyhimi B, Ramakrishna S. Fundamentals and Applications of Micro- and Nanofibers. Cambridge: Cambridge University Press; 2014.